Pharmacological Research 95–96 (2015) 92–101

Contents lists available at ScienceDirect

Pharmacological Research

journal homepage: www.elsevier.com/locate/yphrs

Altered expression of connexin 43 and related molecular partners in a pig model of left ventricular dysfunction with and without dipyrydamole therapy

Silvia Del Ry[a], Stefania Moscato[b], Francesco Bianchi[b], Maria Aurora Morales[a], Amelio Dolfi[b], Silvia Burchielli[c], Manuela Cabiati[a], Letizia Mattii[b,*]

[a] CNR Institute of Clinical Physiology, Laboratory Biochemistry and Molecular Biology, CNR, Italy Clinical Physiology, Pisa, Italy
[b] Department of Clinic and Experimental Medicine, Section Histology, University of Pisa, Pisa, Italy
[c] G Monasterio Foundation, Pisa, Italy

ARTICLE INFO

Article history:
Received 5 November 2014
Received in revised form 23 March 2015
Accepted 23 March 2015
Available online 30 March 2015

Keywords:
Connexin 43
Pig model
Ventricular dysfunction
Dipyridamole
RhoA
Adenosine receptor
Protein kinase C

ABSTRACT

Gap junctions (GJ) mediate electrical coupling between cardiac myocytes, allowing the spreading of the electrical wave responsible for synchronized contraction. GJ function can be regulated by modulation of connexon densities on membranes, connexin (Cx) phosphorylation, trafficking and degradation. Recent studies have shown that adenosine (A) involves Cx43 turnover in A_1 receptor-dependent manner, and dipyridamole increases GJ coupling and amount of Cx43 in endothelial cells. As the abnormalities in GJ organization and regulation have been described in diseased myocardium, the aim of the present study was to assess the regional expression of molecules involved in GJ regulation in a model of left ventricular dysfunction (LVD). For this purpose the distribution and quantitative expression of Cx43, its phosphorylated form pS368-Cx43, PKC phosphorylated substrates, RhoA and A receptors, were investigated in experimental models of right ventricular-pacing induced LVD, undergoing concomitant dipyridamole therapy or placebo, and compared with those obtained in the myocardium from sham-operated minipigs. Results demonstrate that an altered pattern of factors involved in Cx43-made GJ regulation is present in myocardium of a dysfunctioning left ventricle. Furthermore, dipyridamole treatment, which shows a mild protective role on left ventricular function, seems to act through modulating the expression and activation of these factors as confirmed by in vitro experiments on cardiomyoblastic cell line H9c2 cells.

1. Introduction

Gap junctions (GJs) are clusters of transmembrane channels that mediate electrical coupling between cardiac myocytes, allowing the spreading of the electrical wave responsible for synchronized contraction in the heart [1]. These channels consist of two apposing connexon complexes, which allow the direct diffusion of ions and small molecules between adjacent cells [2]. Each connexon comprises six connexin (Cx) proteins, among which the isotype Cx43 is the most widely expressed as well as the most represented in cardiac myocytes gap junctions [3,4].

GJ functions can be regulated at different levels by a variety of mechanisms such as modulation of connexon densities on cell membranes and Cx phosphorylation, which leads to modification of channel conductance as well as Cx trafficking and degradation [5]. Protein kinase C (PKC) has been demonstrated to phosphorylate Cx43 on Ser368 and this state has been shown to induce a reduction in intercellular communication [6]. RhoA, a member of small GTPases, known as key regulator of many cell functions [7], regulates the permeability of Cx43-made GJs in cardiac myocytes [8]. A recent in vitro study has shown that adenosine, an important endogenous physiological modulator of heart function, involves Cx43 turnover in an A_1 receptor-dependent manner [9]. Furthermore, it has recently been demonstrated that the antiplatelet drug dipyridamole increases GJ coupling [10,11] and the amount of Cx43 [12] in smooth muscle and endothelial cells. Increased endogenous adenosine accumulation, achieved with chronic oral

Abbreviations: GJ, gap junction; Cx, connexin; PKC, proteine kinase C; PKCps, phosphorylated PKC substrate; A, adenosine; ARs, adenosine receptor subtypes; LVD, left ventricular dysfunction; RV, right ventricle; LV, left ventricle; LVEDD, left ventricle end diastolic diameter; LVESD, left ventricle end systolic diameter; LVFS, left ventricular fractional shortening; H&E, haematoxylin–eosin; pS368-Cx43, connexin 43 phosphrylated at serina 368; SEM, standard error of the mean.

* Corresponding author at: Department of Clinical and Experimental Medicine, University of Pisa, via Roma 55, Pisa, Italy. Tel.: +39 050 2218615; fax: +39 050 2218620.
E-mail address: letizia.mattii@med.unipi.it (L. Mattii).

http://dx.doi.org/10.1016/j.phrs.2015.03.015
1043-6618/

dipyridamole administration, is known to exert anti-inflammatory, pro-angiogenetic, anti-fibrotic and anti-apoptotic effects, targeting different adenosine receptors subtypes (ARs) (A_1, A_{2A}, A_{2B} and A_3) and cell populations (cardiomyocytes, endothelial cells, leukocytes, cardiac fibroblasts). Thus, a cardioprotective role of this drug in conditions as chronic congestive heart failure has been postulated [13–15].

For the reasons stated above and since the abnormalities in GJ organization and regulation have been implied in different myocardial diseases [1,16,17], the aim of the present study was to assess the regional expression of molecules involved in GJ regulation in a model of left ventricular dysfunction (LVD). For this purpose, the distribution and quantitative expression of Cx43, its phosphorylated form pS368-Cx43, PKC phosphorylated substrates, RhoA and ARs, were investigated in animals with LVD induced by high frequency right ventricular (RV)-pacing. The animals were under concomitant dipyridamole therapy (DP+) or placebo (DP−); sham operated minipigs (C-SHAM) were considered as controls. In addition, the possible dipyridamole signalling transduction pathway was explored by employing the cardiomyoblastic cell line H9c2.

2. Methods

2.1. Experimental animal protocol

Animal instrumentation and experimental protocols were approved by the Animal care Committee according to Italian legislation, following the National Institute of Health publication *Guide for Care and Use of Laboratory Animals*. The experiments were performed according to the guidelines of the European Communities Council Directive 2010/63/EU on the use of animals for scientific purposes.

Twelve minipigs (weight 35–40 kg) were randomly assigned to one of three experimental groups: (1) C-SHAM ($n = 4$), sham operated used as controls, (2) DP+ ($n = 4$), left ventricular dysfunction (LVD) under concomitant dipyridamole therapy (5 mg/kg/daily, Persantin®, Boehringer Ingelheim, Milan, Italy) or (3) DP− ($n = 4$), LVD under placebo therapy. LVD was induced by pacing at 200 bpm in the right ventricular (RV) apex according to previously published protocol [18].

All animals underwent a 2D and M-mode EchoDoppler examination immediately after single chamber pacemaker implantation (t_0) and after 4-weeks (t_4) of RV tachycardic pacing. Then all minipigs were sacrificed with an intravenous injection of 10 ml of KCl and left ventricular (LV) tissue samples were collected according to the guidelines of the American Heart Association [19] after the following sectioning (Fig. 1): from base to the apex, the LV was divided into 16 segments of which six segments in the basal, six segment in the mid portions (anteroseptal, inferoseptal, anterior, anterolateral, inferolateral and inferior walls) and four at the apex (septal, anterior, lateral and inferior walls). In particular, three segments closest to pacing site (8, 9 and 14) and three segments from the opposite site (5, 11 and 12) were collected for this study as reported in a previous published paper [20].

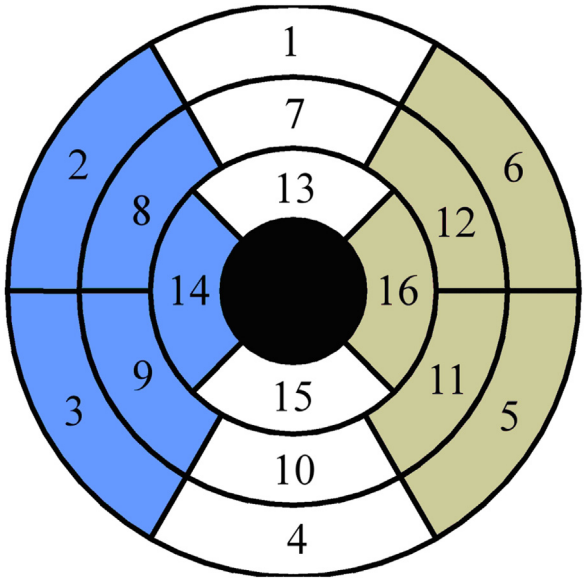

Fig. 1. A circumferential polar plot of the 16 segments (the 17 segment-apex is not considered and is coloured in black) representing the protocol used to group the LV segments in three regions. The septal, adjacent and lateral regions are respectively represented by 2, 3, 8, 9, 14 segments (pacing site), 1, 4, 7, 10, 13, 15 segments and 5, 6, 11, 12, 16 segments (opposite site).

Tissue samples were immediately placed in ice-cold RNAlater (Qiagen, Germany) or 10% formalin solution (Sigma–Aldrich, St. Louis, MO, USA) for following molecular and histological analysis, respectively.

2.2. Echocardiographic examination

Transthoracic echocardiography was performed by one experienced investigator who was blind to underlying treatment using commercially available General Electric Vivid-e equipment. Two dimensional and M-mode data were acquired from the parasternal long and short axis view at the level of papillary muscles and digitally stored for off-line analysis. LV end diastolic diameter (LVEDD), LV end systolic diameter (LVESD) and derived LV fractional shortening (LVFS) were measured in basal conditions (t_0) and after 4 weeks (t_4) pacing.

2.3. Histological analysis

The routinely formalin-fixed and paraffin-embedded LV samples were cut into 8 μ-thick sections, which were serially mounted on glasses. Immediately before use, slides were dewaxed, rehydrated and processed for both routine haematoxylin–eosin (H&E)

Table 1
Antibodies used in this study.

Antibody	Species	Source	Dilution	
			Tissue sections	Cultured cells
Anti-Cx43	Mouse monoclonal	Santa Cruz Biotechnology, Santa Cruz, CA, USA	1:5000	1:200
Anti-phospho-Cx43 (pS368-Cx43)	Rabbit polyclonal	Santa Cruz Biotechnology	1:100	1:50
Anti-RhoA	Mouse monoclonal	ThermoFisher Scientific, Waltham, MA, USA	1:300	
Anti-phospho-PKC substrate (PKCps)	Rabbit polyclonal	Cell Signalling Technology, Beverly, MA, USA	1:600	1:300
Anti-A_{2A}R	Mouse polyclonal	Novus Biological, Cambridge, UK		1:50
Biotinylated anti-mouse immunoglobulins	Goat polyclonal	Vector, Burlingame, CA, USA	1:200	1:200
Biotinylated anti-rabbit immunoglobulins	Goat polyclonal	Vector	1:200	1:200
Alexa Fluor®488 anti-mouse	Goat IgG	Life Technologies Italia, Monza, Italia		1:250
Alexa Fluor®568 anti-rabbit	Donkey IgG	Life Technologies Italia		1:250

Table 2
Primers pairs.

Gene	Primers	Annealing T°	GeneBank
A_1R	5′-ATCAGGTTACTTGGTTCT-3′ 5′-ATCAGGTTACTTGGTTCT-3′	57°	AY772411
$A_{2A}R$	5′-GATCAGCCTCCGCCTCAACGGCCA-3′ 5′-TCAGGACACTCCTGCTCTGTCCTG-3′	60°	AY772412
$A_{2B}R$	5′-TGGTGTACTTCAACTTCCTG-3′ 5′-GATCTTGGCGTAGATGGC-3′	60°	AY772413
A_3R	5′-GGTGAAGTGCCAGAAGTTGTG-3′ 5′-AGCATAGACGATAGGGTTCATCAT-3′	60°	AY772414
RhoA	5′-AGCCCTTACGCGGTTAATTT-3′ 5′-GTGCAGAGGAGGGCTGTTAG-3′	60°	NM_001244437
Cx43	5′-TCCTCCTCTTTCTTGTTCAGTTTCTCT-3′ 5′-CCTGCAGATCATATTTGTGTCTGTTC-3′	59°	AY382593
PPIA	5′-CTTGGGCCGCGTCTCCTTCG-3′ 5′-TTGGGAACCGTTTGTGTTGGGGC-3′	60°	NM_214353
TBP	5′-GATGGACGTTCGGTTTAGG-3′ 5′-AGCAGCACAGTACGAGCAA-3′	60°	DQ178129
YWHAZ	5′-ATGCAACCAACACATCCTATC-3′ 5′-GCATTATTAGCGTGCTGTCTT-3′	60°	DQ178130

Primer pair used for housekeeping and target genes in real time qPCR experiments.
A_1R = adenosine A_1 receptor, $A_{2A}R$ = adenosine A_{2A} receptor, $A_{2B}R$ = adenosine A_{2B} receptor, A_3R = adenosine A_3 receptor, Rho-A = RAS homology family member A, PPIA = cyclophilin A, TBP = TATA-binding protein, YWHAZ = tyrosine 3-monooxygenase/tryptophan 5-monooxygenase activation protein, z polypeptide.

staining and immunohistochemistry. For each cardiac sample, at least 3 serial sections were examined. Immunoperoxidase reactions were performed as previously described [21], using primary and secondary antibodies summarized in Table 1, with respective working dilutions. Sections were counterstained with Harris' haematoxylin (Fluka, Buchs, Switzerland). Negative controls were obtained by omitting primary antibody. Specimens were examined by two independent observers by means of a Leica DMRB light microscope using a semi-quantitative scale of immunoreactivity, consisting of no (−), low (+), medium (++) and high (+++) brown staining. Photomicrographs were taken using a DFC480 digital camera (Leica Microsystem, Cambridge, UK).

2.4. Molecular analysis

Total RNA was extracted by acid guanidinium thiocyanate-phenol-chloroform method from tissue samples obtained from LV tissue with the Rneasy Midi kit (Qiagen S.p.A, Milano, Italy) as previously described [20,22–27].

Purity of total RNA was determined as 260 nm/280 nm absorbance ratio with expected values between 1.8 and 2.1 by the Biophotometer reading (Eppendorf, Italy). Moreover, to check the integrity of 18 and 28 S ribosomal RNAs all samples underwent gel electrophoresis. A known amount of total rat RNA (Ambion) was used as marker. The RNA samples were stored at −80 °C for use in gene expression studies.

Following DNAse treatment, first strand cDNA was synthesized with iScript cDNA Synthesis kit (Bio-rad, Hercules, CA, USA) using about 1 μg of total RNA as template. Reverse transcriptase reaction sequence consisted of incubation at 25 °C for 5 min, followed by three different cycles at 42 °C for 30 min and 45–48 °C for 10 min, in order to better separate the strands. The reverse transcriptase enzyme was inactivated by heating at 85 °C for 5 min. The cDNA samples obtained were placed on ice and stored at 4 °C until further use. Real-Time PCR reactions were performed in duplicate in the Bio-Rad C1000 TM thermal cycler (CFX-96 Real-Time PCR detection systems, Bio-Rad Laboratories Inc., Hercules, CA, USA) as previously described [28]. For monitoring cDNA amplification a third-generation fluorophore, EvaGreen, was used (SsoFAST EvaGreen Supermix, Bio-Rad). PCR was performed in a volume of 20 μl per reaction, including 0.2 μM of each primer (Sigma–Aldrich, St. Louis, MO, USA) samples, reagent and sterile H_2O. Amplification

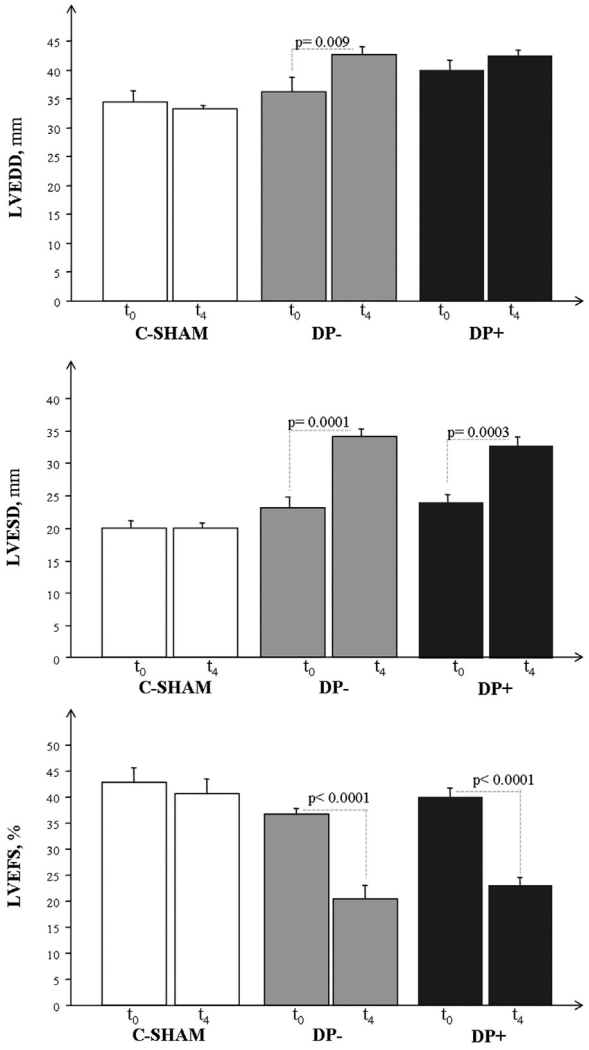

Fig. 2. 2D echocardiographic examination carried out immediately after pacemaker implantation (t_0) and after 4-weeks (t_4) showed LV dysfunction both in DP− and DP+ samples, although DP+ group exhibited a lower LV enlargement respect to DP− group. Each column represents the LVEDD, LVESD and LVFS mean ± SEM (n = 4). $^*p < 0.01$, $^{**}p < 0.001$.

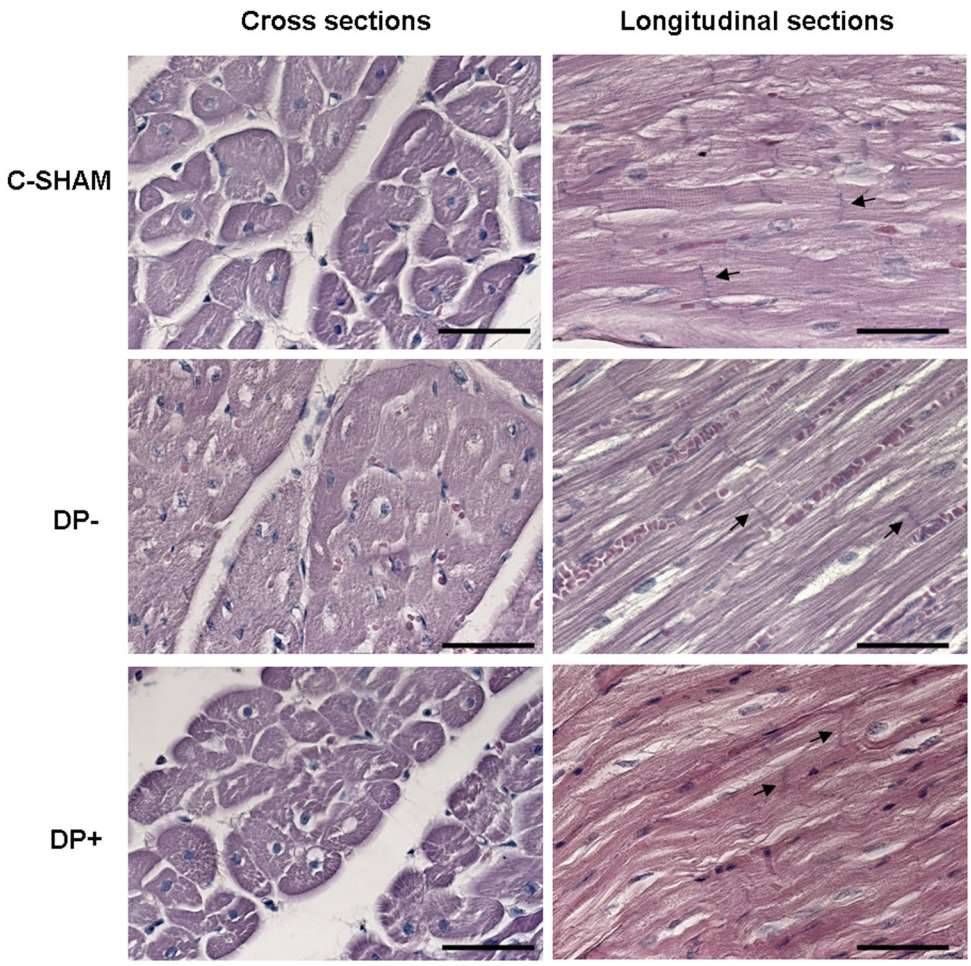

Fig. 3. Optical microscopy analyses in the H&E stained left ventricle sections showed a normal morphology and no differences between the three groups. Arrows indicate intercalated disks. Scale bars represent 50 μm.

protocol started with 98 °C for 30 s followed by 40 cycles at 95 μC for 5 s and 60 °C for 30 s.

Primer pairs were designed with Primer Express Version 2.0 (Applied Biosystems) and details are given in Table 2. Specificity of each primer pair, i.e. the absence of artefacts, multiple PCR products or primer-dimers, and PCR yield was checked by melting analysis.

2.5. Cell culture and experimental protocol

In studies designed to decipher the role of the studied molecules on signalling transduction cascade triggered by dipyridamole we used a rat cardiomyoblast cell line H9c2. The cell line, purchased from the American Tissue Culture Collection (Manasas, VA,USA), was maintained at 37 °C in a humidified atmosphere containing 5% CO_2 in Dulbecco's modified Eagle's Medium (DMEM; Sigma–Aldrich, Schnelldorf, Germany) with 10% foetal bovine serum (FBS; Sigma–Aldrich) and antibiotics (25 U/ml penicillin and 25 U/ml streptomycin, Sigma–Aldrich). For pharmacological experiments, repeated three times, cells were grown on slides and starved for 24 h in DMEM containing 1% FBS and then treated as follows. Dipyridamole at 50 μM was added to cells for 90 min or 24 h [12]. Moreover, cells were pre-treated or not with the $A_{2A}R$ antagonist 8-(3-chlorostyryl)-caffeine (CSC, Sigma–Aldrich) at 10 μM for 30 min [29]. Control samples were obtained incubating cells in 1% FBS/DMEM without both dipyridamole and CSC or with CSC only.

The reactions were stopped fixing cells in 1% formalin/PBS for 10 min at 4 °C. The possible modifications in Cx43, pS368-Cx43, PKCps and $A_{2A}R$ expression were evaluated by immunoperoxidase reactions performed as described in previous 2.3 paragraph with minor changes. Cx43 and pS368-Cx43 were also analyzed by confocal laser scanning microscopy (TC SSP8 Leica Microsystems, Mannheim, Germany) using a 488-nm and 561-nm excitation wavelength lasers. Immunofluorescence reactions were performed using primary antibody and fluorescent secondary antibody at dilutions indicated in Table 1.

2.6. Statistical analysis

For normalization of mRNA expression several reference genes were tested and GeNorm software was used to establish the most stably expressed gene in this experimental setting, as described by Vandesompele et al. [30]. The geometric mean of the three most stably expressed genes was used for normalization of mRNA expression (TBP, YWHAZ, PPIA) (Table 2).

The relative quantification was performed by ΔΔCt method using BioRad's CFX96 manager software. Differences between more than two independent groups were analyzed by Fisher's test after ANOVA. The results are expressed as mean ± SEM and p-value was considered significant when <0.05.

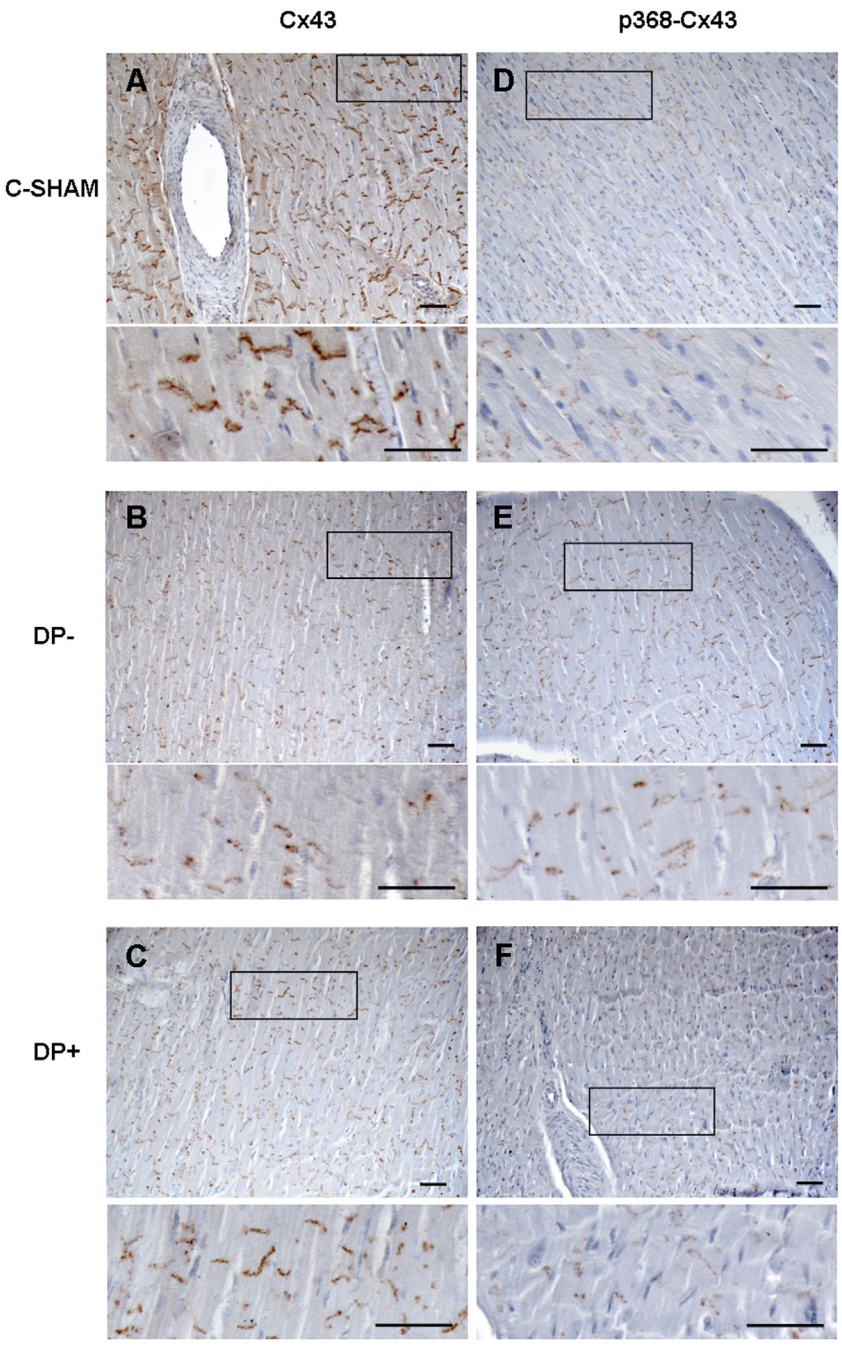

Fig. 4. Immunostaining of LV sections showed appreciable amount of Cx43 in (A) C-SHAM (+++) and a lower Cx43 expression both in (B) DP− (+/++) and (C) DP+ (++) groups. Conversely, p368-Cx43 was more expressed in (E) DP− (+/++) than in (D) DP+ and (F) C-SHAM (+) samples. At higher magnification, it could be noted that Cx43 and its phosphorylated form were localized at level of intercalated disks (blow-up of squares). Scale bars represent 50 μm.

3. Results

3.1. In vivo cardiac 2D echocardiographic examination

As shown in Fig. 2, LVEDD increased from 36 ± 2.5 to 43 ± 1.3 mm ($p = 0.009$) in DP− minipigs when t_0 and t_4 pacing data were compared. In DP+ LVEDD did not increase significantly (from 40 ± 1.6 to 43 ± 1.2 mm). In DP− LVESD increased from 23 ± 1.9 to 34 ± 1.3 mm ($p < 0.0001$) and in DP+ from 24 ± 1.2 to 33 ± 1.3 mm ($p = 0.0003$). Accordingly, LVFS decreased from 37% ± 1.1 to 20% ± 2.5 ($p < 0.0001$) in DP− and from 40% ± 1.7 to 23% ± 1.6 ($p < 0.0001$) in DP+. No changes were observed in the C-SHAM group for all the considered parameters (LVEDD from 34 ± 1.8 to 33 ± 10.6 mm, LVESD from 20 ± 1.5 to 20 + 1.1 mm; LVFS: from 43% ± 2.8 to 41% ± 2.8).

3.2. Histological and molecular analysis of pig LV samples

Left ventricular cardiac tissue from 3 experimental group samples showed a normal morphology as observed on H&E stained sections. The working contractile myocytes revealed in all sections no differences in size and myofibril array (Fig. 3).

Immunohistological analysis showed that all antigens under study were expressed in the 3 groups as a brown reaction undetected in negative controls. No differences in immunoreactivity for all antigens were found between the 6 regions collected from LV

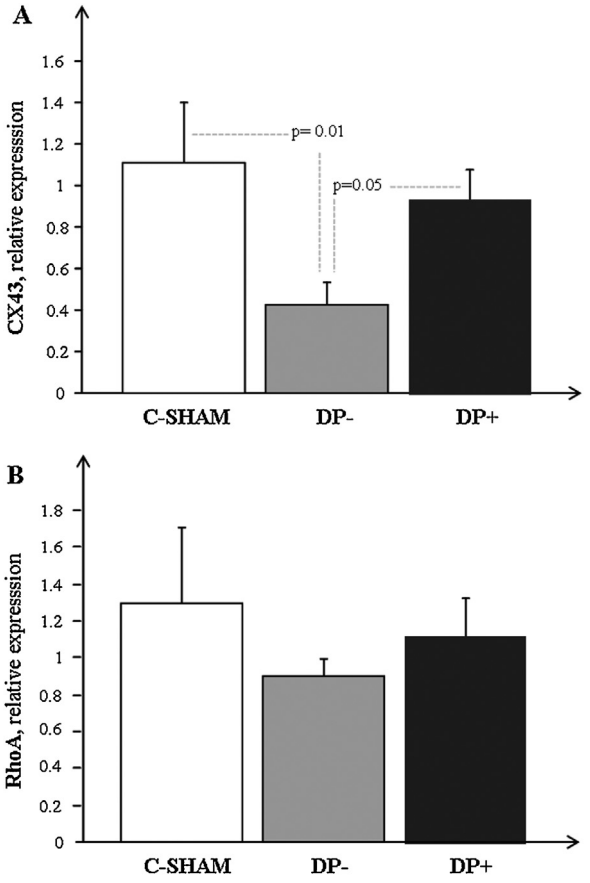

Fig. 5. mRNA expression of (A) Cx43 and (B) RhoA in C-Sham (white bar), DP− (grey bar) and DP+ (black bar) LV minipigs.

of each minipig for all antigens. Moreover, no differences in mRNA amount could be reported between these regions. Despite these findings, significant abnormalities concerning the expression of the investigated molecules were found in the LVD samples.

3.3. Cx43 expression

A remarkable amount of Cx43 immunostaining (+++) was detected in control samples where Cx43 appeared localized to intercalated disks (Fig. 4A). In DP− and DP+ samples the Cx43 positivity was still distributed to intercalated disks but it was heavily reduced in DP− (+/++) or slightly reduced in DP+ (++/+++) (Fig. 4B and C). The expression of Cx43 mRNA, determined by Real Time PCR, was reduced only in the DP− samples, which showed significant differences when compared to the C-SHAM and DP+ samples (Fig. 5A).

Cx43 phosphorylated at S368 (pS368-Cx43) was detected by immunohistochemistry and localized at the intercalate disks in all samples at low level (+) in the control and DP+ samples (Fig. 4D and F) and at higher level (++) in DP− samples (Fig. 4E). The expression of pS368-Cx43 matched with total Cx43 expression in DP− group while it was lower than total Cx43 in DP+ groups and much lower in C-SHAM groups.

3.4. RhoA, PKCps and ARs expression

With regard to RhoA, a strong immunolabelling (+++, Fig. 6) was detected in all samples at the level of contractile myocytes, vessel smooth muscle cells and endothelial cells, and no differences were observed between the groups both in protein and mRNA expression (Fig. 5B). However, at higher magnification myocytes of control and DP+ samples showed a RhoA immunopositivity mostly localized in the cytoplasm while those of DP− samples presented RhoA reactivity distributed especially at plasma membrane level (Fig. 6B, arrows). Interestingly, the cellular localization of RhoA corresponds to its metabolic state: cytoplasmic or plasma membrane staining corresponding to inactivated GDP-bound or activated GTP-bound RhoA, respectively [31–33].

The activity of PKC was indirectly studied through the levels of phosphorylated PKC substrates (PKCps). A weak PKCps immunostaining (+) was detected in all samples at the level of intercalated disks. On the other hand, while only few intercalated disks were reactive in control and DP+ samples (Fig. 7A–C), a more substantial number was positive in DP− ones (Fig. 7B).

As far as adenosine receptors, A_1R, $A_{2B}R$ and A_3R mRNA expression resulted significantly reduced in DP− and DP+ samples when compared with C-SHAM, while $A_{2A}R$ resulted significantly increased in DP+ with respect to C-SHAM and DP− samples (Fig. 8).

3.5. Dipyridamole treatment and $A_{2A}R$ inhibition in H9c2 cells

The treatment of H9c2 cells with 50 μM dipyridamole enhanced Cx43 expression both after 90 min (++) (Fig. 9A, B, D and E) and 24 h (+++), as compared to control cells (+). In particular, as showed by 3D confocal images, in control cells the light immunopositivity was focused in the cytoplasm region around nucleus, while in DP treated cells marked immunopositivity extended to periferic cytoplasm and membrane (Fig. 9D and E). On the contrary, the expression of Cx43 phosphorylated at S368 decreased after dipyridamole treatment: appreciable immunoreaction (++) was localized both at nuclear and at plasma membrane level in control cells while little immunoreactivity (+) was observed in DP treated cells (Fig. 9D and E)

The activity of PKC, documented by the expression of PKC phosphorylated substrates, was clearly decreased after both 90 min (++) (Fig. 10A and B) and 24 h (++) of dipyridamole incubation respect to controls (+++). $A_{2A}R$ immunopositivity resulted increased after 24 h dipyridamole treatment (++) (Fig. 10D and E) but not after 90 min respect to controls (+). The pre-treatment with CSC, a selective $A_{2A}R$ receptor antagonist, prevented the changes on Cx43, pS368-Cx43, PKCps and $A_{2A}R$ expression induced by dipirydamole. In fact, as observed in the representative images of Fig. 9C and F and Fig. 10C and F the immunopositivity of H9c2 cells pre-treated with CSC resembled those of controls. Control cells whether incubated in 1% FBS/DMEM without dipyridamole and CSC or treated with CSC alone showed the same immunopositivity (data not shown).

4. Discussion

Cx43, a predominant connexin in the heart, abundant in ventricular cardiomyocytes, forms GJs that facilitate electrical cell–cell coupling and hemichannels that represent a pathway for the exchange of ions and metabolites between cytoplasm and the extracellular milieu [3, 4 and 34]. Abnormalities in the Cx43 expression, localization and phosphorylation status were found in the setting of myocardial ischaemia and atrial-ventricular arrhythmias [1,17].

In the current study, the expression of Cx43 and some of its regulatory molecules were evaluated in the LV myocardium of minipigs with pacing-induced LVD, with or without concomitant dipyridamole therapy, as well as in the LV of healthy sham operated minipigs.

The model of LVD induced by RV pacing is well known in experimental animal models. Pacing at the right ventricular apex reduces LV function more than pacing at the high ventricular septum or at

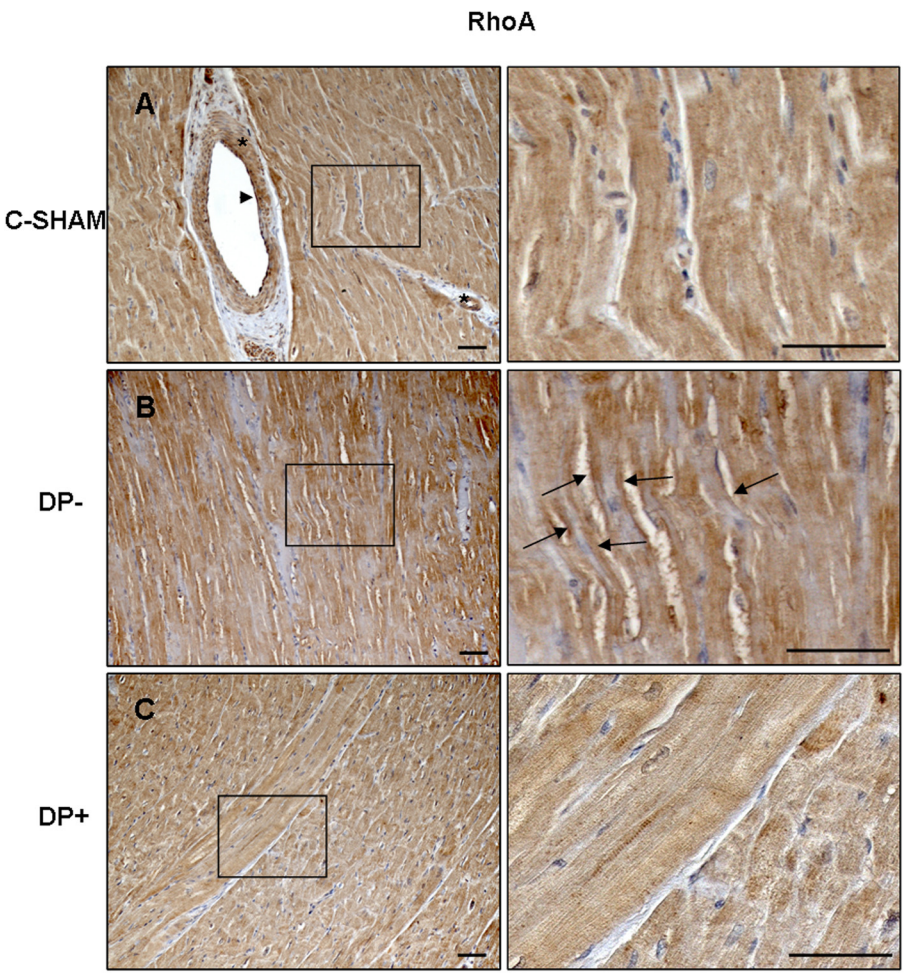

Fig. 6. Strong RhoA immunolabelling (+++) was detected in all LV samples in myocytes, smooth muscle cells (asterisk) and endothelial cells (arrowhead) of (A) C-SHAM, (B) DP− and (C) DP+, without differences between the groups. However, higher magnification showed RhoA mainly distributed at membrane level in DP− samples (B, arrows in blow-up of square) compared with C-SHAM and DP+ samples where RhoA was mainly localized at cytoplasm level ((A, C), blow-up of squares). Scale bars represent 50 μm.

LV sites, likely due to the combination of the effects of dyssynchrony (due to RV apical pacing) and tachycardia, without potential interference on LV myocardium due to the electrocatheter positioning [35]. Interestingly, in this model, we did not found regional differences in morphology and expression of studied molecules, as demonstrated by the similar results obtained by histological and molecular analysis in the segments from both close to the pacing site and those from opposite site of each LV. These results could be possibly explained by the lack of myocardial damage observed, on the contrary, when the electrocatheter is positioned in the LV myocardium. In fact, in this case regional LV differences in adenosine receptor expression have been reported [23].

Echocardiographic examination at t_0 and t_4 on minipigs from the 3 groups clearly demonstrated LV dysfunction. In fact, DP− and DP+ groups showed an increase of LVEDD and LVESD with a consequent reduction of LVFS. Dipyridamole therapy seemed to partially preserve myocardial function since LV dilatation was less evident and a marginally better LVFS percentage was also reported in DP+ as compared to DP− animals.

In this model, no evident histo-morphological alterations were induced, as observed in H&E sections, while clear differences in the expression/activation of Cx43 and its partner molecules among the three groups of minipigs were evidenced with the immunohistochemical and molecular biology analysis. In fact, Cx43 expression, both at protein and mRNA level, was more reduced after 4 weeks of pacing in DP− LV samples when compared with C-SHAM samples. As Cx43 has a relatively short half-life, in the order of 1–2 h [36], it could be hypothesized that both synthesis and degradation of this protein are among the major mechanisms involved in gap junction regulation. Moreover, Cx43 phosphorylation on Ser368, mediated by PKC, leads to a decrease in GJ communication [6], probably by increased internalization and degradation through lysosomal and/or proteasomal pathway [37]. It is to note that in our DP− group the expression of pS368-Cx43 matched with total Cx43 expression. Therefore, in our DP− samples, the reduced Cx43 protein expression could be due to both decreased Cx43 synthesis, as demonstrated by a reduced Cx43 mRNA, and increased Cx43 PKC-induced phosphorylation, as suggested by the increase of both p368Cx43 and PKC phosphorylated substrates expression. Based on the role traditionally ascribed to GJs, the dramatic reduction of Cx43 expression found in DP− samples could be related to impaired junctional communications among adjacent cardiomyocytes leading to a reduction of electrical conduction. On the other hand, Cx43 reduction could also correspond to a loss of Cx43 hemichannels with consequent cardioprotective effect. In fact, emerging evidence has suggested that the block of unapposed/nonjunctional hemichannels residing in the zone surrounding the GJ area, could confer cardioprotection by preventing ionic imbalance, cell swelling and loss of metabolites [34]. Furthermore, when considering the increased activation of RhoA in DP− samples, as demonstrated by its high content at level of plasma membrane, this pathway could enhance the

processes of cell-to-cell solute diffusion, without interfering with the cellular redistribution of junctional plaques or the Cx43 phosphorylation pattern [8]. Therefore, RhoA could be involved in a compensatory action restoring junctional communications among cardiomyocytes. High PKC activation observed in these samples could activate RhoA pathway as reported in foetal cerebral arteries but not in adult [38]. Alternative RhoA rules cannot be excluded since, even though in the contest of myocardium, the role of RhoA/ROCK pathway is less well understood than its role in the vasculature, there is growing evidence that it plays an important pathophysiological role in cardiovascular diseases, likely through the effects on cytoskeleton organization, cell growth and development, and transcriptional regulation [39].

With regard to the molecular effect of dipyridamole, we found that LV cardiomyocytes of LVD minipigs responded to 4-weeks dipyridamole treatment by increasing Cx43 mRNA and protein expression with concomitant reducing of p368Cx43 expression and PKC activation as compared with DP− samples. These results were rather similar to that of control samples suggesting that dipyridamole tends to restore a molecular pattern of control. As dipyridamole enhanced adenosine function by the inhibition of nucleoside transporters [40], we suppose that it could modulate Cx43 expression via adenosine/A_{2A} receptor pathway. In fact, when we investigated ARs expression we found an increase of A_{2A}R mRNA only in DP+ with respect to DP− samples and control. Interestingly we demonstrated that dipyridamole enhanced A_{2A}R expression also in the H9c2 cell line, valuable in vitro model to heart studies [41], and that A_{2A}R activation is a prerequisite for the effects of dipyridamole. In fact, the pretreatment with the CSC antagonist of A_{2A}R on H9c2 abolished the effects of dipyridamole on Cx43, p368Cx43, PKCps and A_{2A}R expression. The involvement of ARs in the turnover of Cx43 has been recently demonstrated in vitro in a

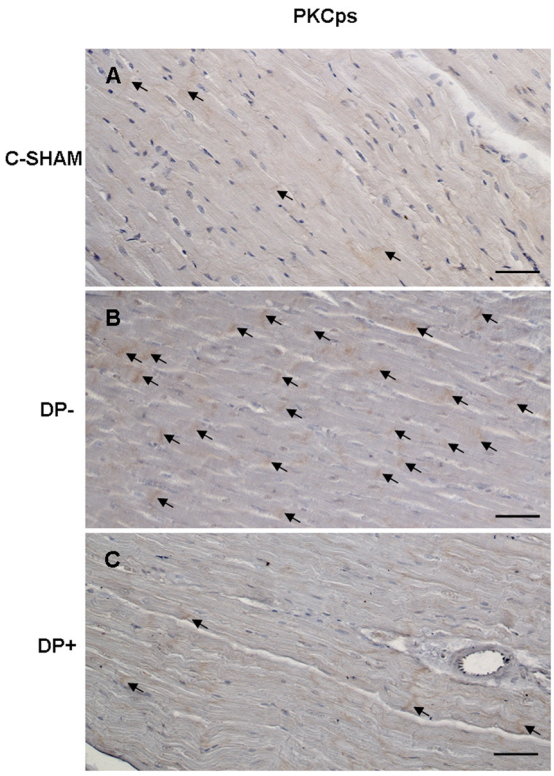

Fig. 7. Weak PKCps immunostaining of LV sections was detected in (A) C-SHAM, (B) DP−, (C) DP+ at intercalated disks (+, arrows), although much more disks were reactive in DP− samples (B) as compared with control and DP+ samples (A, C). Scale bars represent 50 μm.

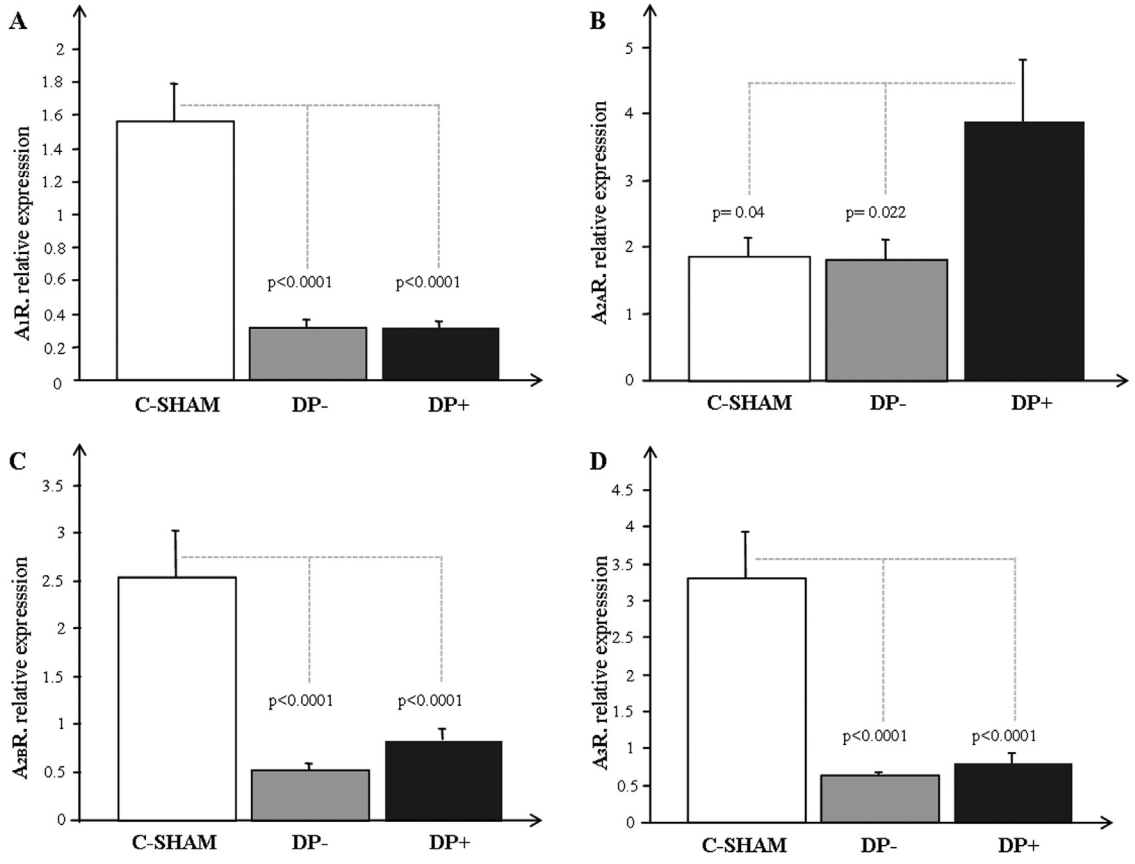

Fig. 8. mRNA expression of (A) A_1R, (B) A_{2A}R, (C) A_{2B}R and (D) A_3 R in C-SHAM (white bar), DP− (grey bar) and DP+ (black bar) LV minipigs.

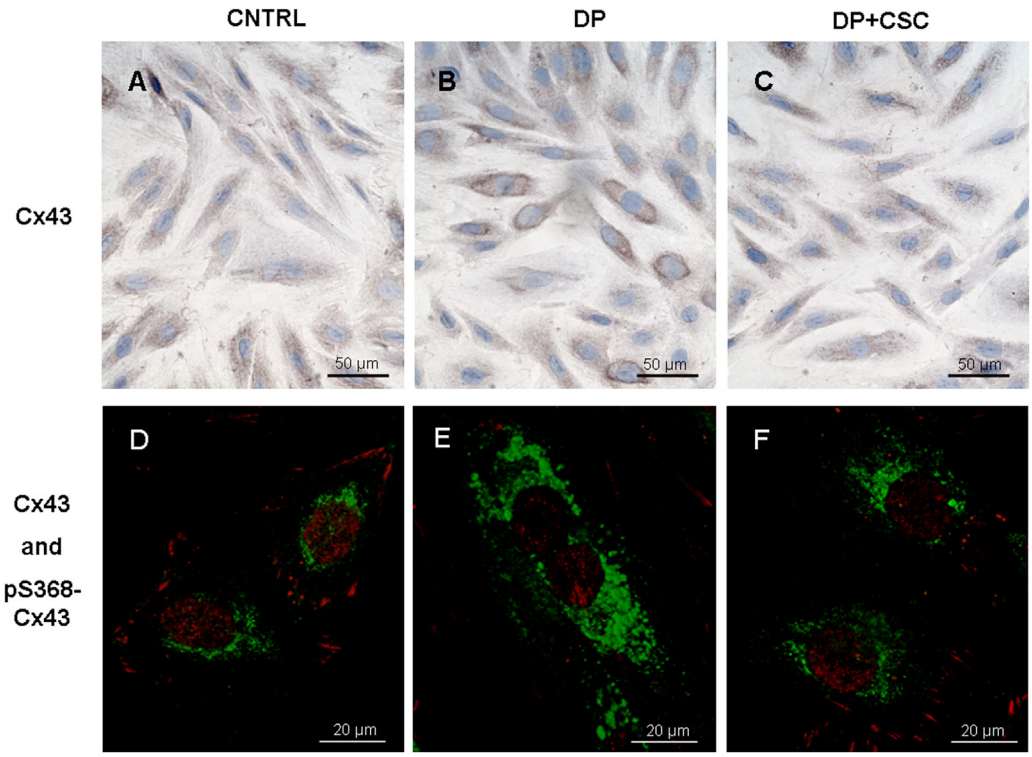

Fig. 9. Effect of dipyridamole and CSC on the expression of Cx43 and pS368-Cx43. Representative examples of immunoperossidase (A–C) and immunofluorescence (D–F) performed on H9c2 of control (A, D), treated for 90 min with DP without (B, E) or with (C, F) CSC pre-treatment. The 3D images (D–F) resulted from the maximum projection of 25–30 images collected at 0.25 μm steps in the *z* axis. Cx43 and pS368-Cx43 are represented by green or red reaction, respectively.

cellular model of cardiac hypertrophy induced by isoproterenol. In particular, the authors suggested that adenosine/A_1R pathway was involved in the PKC-induced decreased level of Cx43 [9]. On the contrary, we found that in DP– and DP+ samples A_1R, A_{2B}R, A_3R were down-expressed with respect to controls. These ARs results are not totally in agreement with our previous studies [22–24] showing generally an up-regulation of ARs in different pig models of heart failure. The ARs down-regulation could be ascribed to a desensitization caused by higher adenosine concentration [42] but this mechanism deserves further exploitations. However, the

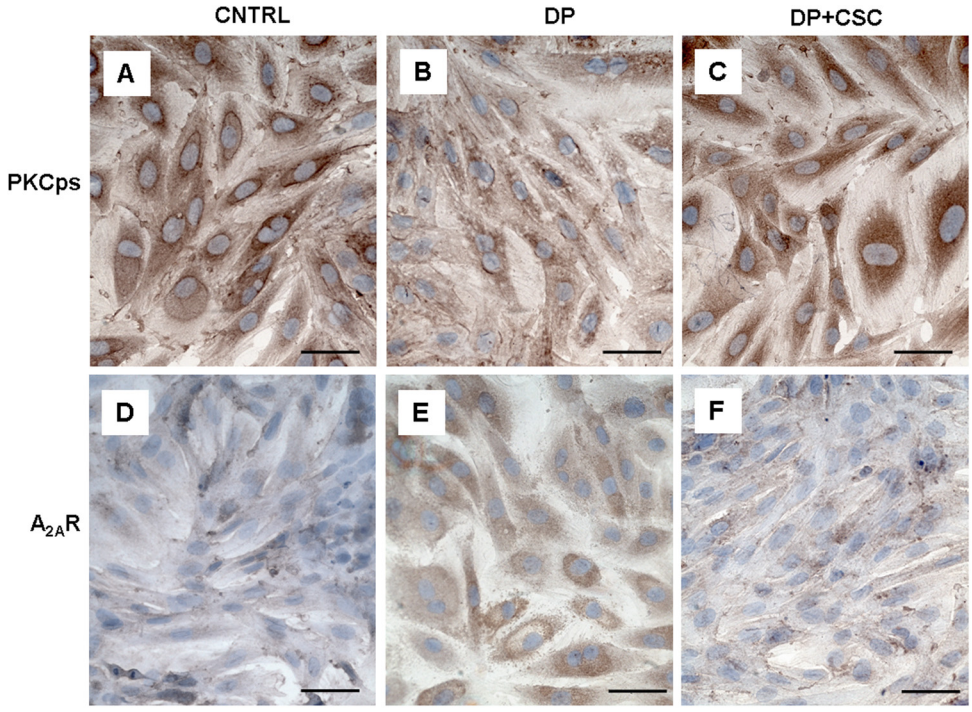

Fig. 10. Effect of dipyridamole and CSC on the expression of PKCps and A_{2A}R. Representative examples of immunoperossidase performed on H9c2 of control (A, D), treated with DP for 90 min (B) or 24 h (E) and with DP + CSC (C, F). Scale bars represent 50 μm.

different modality of LV dysfunction performed in this study might account for this discrepancy.

In conclusion, despite the small number of animal studied, this preliminary study shows that an altered expression of Cx43 and changes in its regulatory factors are present in the setting of LVD in minipigs model. Moreover, for the first time, it shows that dipyridamole influences Cx43 expression and its regulation at level of contractile cardiomyocytes likely through AR/PKC pathway. The characterization of the signal transduction pathways involved in Cx43 expression in myocardium could represent a potential tool for a better comprehension of the mechanisms underlying LVD in absence of coronary or valvular disease.

Acknowledgements

The paper was partially supported by University of Pisa. The authors would like to thank Mr. Sauro Dini, Dr. Chiara Ippolito and Dr. Cristina Segnani for skilful technical support.

References

[1] N.J. Severs, A.F. Bruce, E. Dupont, S. Rothery, Remodelling of gap junctions and connexin expression in diseased myocardium, Cardiovasc. Res. 80 (2008) 9–19.
[2] D.A. Goodenough, J.A. Goliger, D.L. Paul, Connexins, connexons, and intercellular communication, Annu. Rev. Biochem. 65 (1996) 475–502.
[3] D.B. Gros, H.J. Jongsma, Connexins in mammalian heart function, Bioessays 18 (1996) 719–730.
[4] N.J. Severs, S. Rothery, E. Dupont, S.R. Coppen, H.I. Yeh, Y.S. Ko, et al., Immunocytochemical analysis of connexin expression in the healthy and diseased cardiovascular system, Microsc. Res. Tech. 52 (2001) 301–322.
[5] D.A. Goodenough, D.L. Paul, Gap junctions, Cold Spring Harb. Perspect. Biol. 1 (2009), a002576, 1–19.
[6] J.F. EK-Vitorin, T.J. King, N.S. Heyman, P.D. Lampe, J.M. Burt, Selectivity of connexin 43 channels is regulated through protein kinase C-dependent phosphorylation, Circ. Res. 98 (2006) 1498–1505.
[7] A. Hall, Rho GTOases and control of cell behaviour, Biochem. Soc. Trans. 33 (2005) 891–895.
[8] M. Derangeon, N. Bourmeyster, I. Plaisance, C. Pinet-Charvet, Q. Chen, F. Duthe, et al., RhoAGTPase and F-actin dynamically regulate the permeability of Cx43-made channels in rat cardiac myocytes, J. Biol. Chem. 283 (2008) 30754–30765.
[9] A. Popolo, S. Morello, R. Sorrentino, A. Pinto, Antiadrenergic effect of adenosine involves connexin 43 turn-over in H9c2 cells, Eur. J. Pharmacol. 715 (2013) 56–61.
[10] D. Begandt, W. Bintig, K. Oberheide, S. Schlie, A. Ngezahayo, Dipyridamole increases gap junction coupling in bovine GM-7373 aortic endothelial cells by a cAMP-protein kinase A dependent pathway, J. Bioenerg. Biomembr. 42 (2010) 79–84.
[11] D. Begandt, A. Bader, L. Dreyer, N. Eisert, T. Reeck, A. Ngezahayo, Biphasic increase of gap junction coupling induced by dipyridamole in the rat aortic A-10 vascular smooth muscle cell line, J. Cell Commun. Signal. 7 (2013) 151–160.
[12] D. Begandt, A. Bader, L. Gerhard, J. Lindner, L. Dreyer, B. Schlingmann, et al., Dipyridamole-related enhancement of gap junction coupling in the GM-7373 aortic endothelial cells correlates with an increase in the amount of connexin 43 mRNA and protein as well as gap junction plaques, J. Bioenerg. Biomembr. 45 (2013) 409–419.
[13] M. Kitakaze, T. Minamino, K. Node, Y. Koretsune, K. Komamura, H. Funaya, et al., Elevation of plasma adenosine levels may attenuate the severity of chronic heart failure, Cardiovasc. Drugs Ther. 12 (1998) 307–309.
[14] H. Funakoshi, L.C. Zacharia, Z. Tang, J. Zhang, L.L. Lee, J.C. Good, et al., A1 adenosine receptor upregulation accompanies decreasing myocardial adenosine levels in mice with left ventricular dysfunction, Circulation 115 (2007) 2307–2315.
[15] S.A. Epperson, L.L. Brunton, I. Ramirez-Sanchez, F. Villarreal, Adenosine receptors and second messenger signaling pathways in rat cardiac fibroblasts, Am. J. Physiol. Cell Physiol. 296 (2009) C1171–C1177.
[16] A. Salameh, S. Krautblatter, S. Karl, K. Blanke, D.R. Gomez, S. Dhein, et al., The signal transduction cascade regulating the expression of the gap junction protein connexin43 by beta-adrenoceptors, Br. J. Pharmacol. 158 (2009) 198–208.
[17] J.H. Smith, C.R. Green, N.S. Peters, S. Rothery, Severs. Altered patterns of gap junction distribution in ischemic heart disease. An immunohistochemical study of human myocardium using laser scanning confocal microscopy, N. J. Am. J. Pathol. 139 (1991) 801–821.
[18] G.W. Moe, P. Armstrong, Pacing-induced heart failure: a model to study the mechanism of disease progression and novel therapy in heart failure, Cardiovasc. Res. 42 (1999) 591–599.
[19] M.D. Cerqueira, N.J. Weissman, V. Dilsizian, A.K. Jacobs, S. Kaul, W.K. Laskey, et al., Standardized myocardial segmentation and nomenclature for tomographic imaging of the heart. A statement for healthcare professionals from the cardiac imaging committee of the council on clinical cardiology of the American Heart Association, Circulation 105 (2002) 539–542.
[20] M. Cabiati, S. Burchielli, M. Matteucci, B. Svezia, L. Panchetti, C. Caselli, et al., Dipyridamole-induced C-type natriuretic peptide mRNA overexpression in a minipig model of pacing-induced left ventricular dysfunction, Peptides 19 (64C) (2015) 67–73.
[21] L. Mattii, C. Ippolito, C. Segnani, B. Battolla, R. Colucci, A. Dolfi, et al., Altered expression pattern of molecular factors involved in colonic smooth muscle functions: an immunohistochemical study in patients with diverticular disease, PLoS ONE 8 (2013) e57023.
[22] S. Del Ry, M. Cabiati, A. Martino, A. Simioniuc, M.A. Morales, E. Picano, Adenosine receptor mRNA expression in normal and failing minipig hearts, J. Cardiovasc. Pharmacol. 58 (2011) 149–156.
[23] S. Del Ry, M. Cabiati, V. Lionetti, G.D. Aquaro, A. Martino, L. Mattii, et al., Pacing-induced regional differences in adenosine receptors mRNA expression in a swine model of dilated cardiomyopathy, PLoS ONE (2012) 7e47011.
[24] M. Cabiati, A. Martino, L. Mattii, C. Caselli, T. Prescimone, V. Lionetti, et al., Adenosine receptor expression in an experimental animal model of myocardial infarction with preserved left ventricular ejection fraction, Heart Vessels 29 (2013) 513–529.
[25] S. Del Ry, M. Cabiati, V. Lionetti, C. Colotti, M. Maltinti, M. Emdin, et al., Sequencing and cardiac expression of natriuretic peptide receptor 2 (NPR-B) in Sus Scrofa, Peptides 28 (2007) 1390–1396.
[26] S. Del Ry, M. Cabiati, V. Lionetti, M. Emdin, F.A. Recchia, D. Giannessi, Expression of C-type natriuretic peptide and of its receptor NPR-B in normal and failing heart, Peptides 29 (2008) 2008–2015.
[27] S. Del Ry, M. Cabiati, V. Lionetti, A. Simioniuc, C. Caselli, T. Prescimone, et al., Asymmetrical myocardial expression of natriuretic peptides in pacing-induced heart failure, Peptides 30 (2009) 1710–1713.
[28] M. Cabiati, S. Raucci, C. Caselli, M.A. Guzzardi, A. D'Amico, T. Prescimone, et al., Tissue-specific selection of stable reference genes for real-time PCR normalization in an obese rat model, J. Mol. Endocrinol. 48 (2012) 251–260.
[29] T. Pang, X.T. Gan, D.J. Freeman, M.A. Cook, M. Karmazyn, Compensatory upregulation of the adenosine system following phenylephrine-induced hypertrophy in cultured rat ventricular myocytes, Am. J. Physiol. Heart Circ. Physiol. 298 (2010) H545–H553.
[30] J. Vandesompele, K. De Preter, F. Pattyn, B. Poppe, N. Van Roy, A. De Paepe, et al., Accurate normalization of real-time quantitative RT-PCR data by geometric averaging of multiple internal control genes, Genome Biol. (2002), research0034.1–.11.
[31] A. Hall, Rho GTPases and the actin cytoskeleton, Science 279 (1998) 509–514.
[32] L. Mattii, B. Battolla, A. Azzarà, G. D'Urso, U. Montali, M. Petrini, Glycosylation interference on RhoA activation: focus on G-CSF, Leuk. Res. F35 (2011) 265–267.
[33] L. Mattii, R. Fazzi, S. Moscato, C. Segnani, S. Pacini, S. Galimberti, et al., Carboxy-terminal fragment of osteogenic growth peptide regulates myeloid differentiation through RhoA, J. Cell. Biochem. 15 (2004) 1231–1241.
[34] N. Wang, E. De Vuyst, R. Ponsaerts, K. Boengler, N. Palacios-Prado, J. Wauman, et al., Selective inhibition of Cx43 hemichannels by Gap19 and its impact on myocardial ischemia/reperfusion injury, Basic Res. Cardiol. 108 (2013) 309.
[35] T.T. Vo Thang, B. Thibault, V. Finnerty, M. Pelletier-Galarneau, P. Khairy, J. Grégoire, F. Harel, Canine left ventricle electromechanical behavior under different pacing modes, Electrophysiol 35 (2012) 11–17.
[36] D.W. Laird, Life cycle of connexins in healty and disease, Biochem. J. 394 (2006) 527–543.
[37] E. Leithe, E. Rivedal, Ubiquitination of gap junction proteins, J. Membr. Biol. 217 (2007) 43–51.
[38] R. Goyal, A. Mittal, N. Chu, L. Shi, L. Zhang, L.D. Longo, Maturation and the role of PKC-mediated contractility in ovine cerebral arteries, Am. J. Physiol. Heart Circ. Physiol. 297 (2009) H2242–H2252.
[39] M. Surma, L. Wei, J. Shi, Rho kinase as a therapeutic target in cardiovascular disease, Future Cardiol. 7 (2011) 657–671.
[40] M. Molina-Arcas, F.J. Casado, M. Pastor-Anglada, Nucleoside transporter proteins, Curr. Vasc. Pharmacol. 7 (2009) 426–434.
[41] B.N. Zordoky, A.O. El-Kadi, H9c2 cell line is a valuable in vitro model to study the drug metabolizing enzymes in the heart, J. Pharmacol. Toxicol. Methods 56 (2007) 317–322.
[42] F. Ciruela, C. Saura, E.I. Canela, J. Mallol, C. Lluís, R. Franco, Ligand-induced phosphorylation, clustering, and desensitization of A1 adenosine receptors, Mol. Pharmacol. 52 (1997) 788–797.